ELSEVIER

Gas phase molecular spectroscopy/Spectroscopie moléculaire en phase gazeuse

Photoassociation spectroscopy of ultra-cold long-range molecules

Nicolas Vanhaecke, Daniel Comparat, Anne Crubellier, Pierre Pillet *

Laboratoire Aimé Cotton, CNRS II, bâtiment 505, campus d'Orsay, 91405 Orsay cedex, France

Presented by Guy Laval

Abstract

Spectroscopic study of so-called long-range molecules, with average interatomic distances much larger than usual for chemical bonds, is conveniently performed by photoassociation (PA) of ultracold atoms. We present here a review of our results obtained by one and two-photon PA spectroscopy of the Cs_2 molecule, using as intermediate the 0_g^- and 1_u potentials correlated to the $(6s + 6p_{3/2})$ asymptote. These results have been interpreted using an asymptotic theoretical approach, which was specifically build for such long-range molecules. ***To cite this article: N. Vanhaecke et al., C. R. Physique 5 (2004).***
© 2004 Académie des sciences. Published by Elsevier SAS. All rights reserved.

Résumé

Spectroscopie par photoassociation d'atomes ultra-froids de molécules de grande élongation. La spectroscopie des molécules dites « de grande élongation », pour lesquelles la distance interatomique est considérablement plus grande qu'elle ne l'est habituellement dans la liaison chimique peut être réalisée par photoassociation d'atomes ultra-froids. Nous présentons ici une synthèse des résultats obtenus par spectroscopie de photoassociation à un et à deux photons pour la molécules de Cs_2. Les potentiels excités concernés sont les potentiels 0_g^- et 1_u, corrélés à la limite asymptotique $(6s + 6p_{3/2})$. Tous les résultats obtenus ont été interprétés dans une approche théorique asymptotique, spécialement développée pour l'étude de ces molécules de grande élongation. ***Pour citer cet article : N. Vanhaecke et al., C. R. Physique 5 (2004).***
© 2004 Académie des sciences. Published by Elsevier SAS. All rights reserved.

1. Introduction

The development of laser-cooling techniques for atoms has given rise to powerful high resolution molecular spectroscopy, via the photoassociation of ultracold atoms, first suggested in [1]. This spectroscopy opened a novel field, the study of so-called long-range molecular states, with elongations much larger than it is usual for molecular states, that are quite difficult to reach by standard ways. Such a study required the development of new theoretical approaches, focusing on the asymptotic part of the molecular potentials, that is at the frontier between atomic and molecular physics. Conversely it yielded accurate new information about the asymptotic part of the molecular potentials. From our cesium experiments, we obtained for instance the coefficient of the $6s$–$6p$ dipole–dipole interaction, which provides an accurate determination of the $6p_{1/2}$ and $6p_{3/2}$ atomic lifetimes, and also a precise value of the C_6 van der Waals coefficient of the Cs_2 ground state, which is crucial for the determination of collisional properties such as scattering lengths.

1.1. Photoassociation spectroscopy

In a photoassociation (PA) process a pair of colliding ultracold atoms absorbs resonantly one laser photon to form an electronically excited molecule in some ro-vibrational level (v, J). In the case of a pair of cesium atoms and for the first electronically excited states (the system specifically considered in this article), the reaction can be expressed

$$\mathrm{Cs}(6s, F) + \mathrm{Cs}(6s, F) + h\nu_L \to \mathrm{Cs}_2\big(\Omega(6s + 6p_j); v, J\big), \tag{1}$$

where F is the hyperfine level of the atomic ground state, ν_L is the laser frequency, which is red-detuned from the atomic frequency ($6s \to 6p_j$, $j = 1/2$ or $3/2$). The symbol Ω denotes an excited molecular sate correlated to one of the excited asymptotes, either $(6s + 6p_{1/2})$ or $(6s + 6p_{3/2})$. The resolution of the PA process is limited by the width of the statistical distribution of the relative kinetic energy of the colliding atoms, which is of the order of $k_B T$ (k_B is the Boltzmann constant and T the temperature of the atomic sample). The extremely narrow width of the thermal distribution of ultracold atoms ($k_B T \sim h \times 2$ MHz at $T \sim 100$ μK), smaller than any other relevant energy of the system such as the molecular level spacing, allows one to reach high resolution. PA spectroscopic studies (for a review see [2,3]) have been performed for all alkali atoms from Li to Cs: the first studies were for Na$_2$ [4], followed by Rb$_2$ [5], Li$_2$ [6], K$_2$ [7], and Cs$_2$ [8]. PA has been further demonstrated for hydrogen [9], then metastable helium [10,11] and calcium [12] have been photoassociated too. Preliminary results for heteronuclear alkali systems have also been reported [13,14] and RbCs has been recently photoassociated [15]. PA spectroscopy gives access to the previously unexplored domain of molecular dynamics at distances well beyond those usually associated with chemical bonds.

PA process not only offers a novel technics for the molecular spectroscopy, but, as it will be explained below, it also allows us to form ultracold molecules in the ground-state [8]. PA processes involving several laser frequencies, so-called multi-photon PA processes, have also been worked out in cold atomic samples, both in ladder-like [16] and Λ-like schemes [6,17,18]. A theoretical treatment of one and two-colour PA spectroscopy has been presented in [19]. The richness of two-colour lineshapes (Fano profiles, optical Feshbach resonances) has been demonstrated in Cs experiment [20].

1.2. Long-range alkali dimer: a pair of atoms

The concept of 'pure long-range molecules', in which the relative motion of the two atoms takes place mainly at large interatomic distances, so that only electrostatic interactions are important, any chemical interaction being negligible, was introduced by Stwalley et al. [21]. An example is given in Fig. 1, where the potential curves representing the interaction of a pair of ground-state cesium atoms and of a pair of $\mathrm{Cs}(6s) + \mathrm{Cs}(6p_{1/2 \text{ or } 3/2})$ atoms are shown. Due to the dipole–dipole R^{-3} asymptotic interaction, the excited curves extend at much more larger range than the ground-state curves which presents an asymptotic R^{-6} behavior. This feature is general for homonuclear dimers, but not for heteronuclear dimers where the excited curves display a R^{-6} long range behavior. The long-range R^{-3} behavior implies the existence of vibrational levels with very large elongation, up to a few hundreds of atomic units. In the cesium case, PA of cold atoms has allowed us to reach ro-vibrational levels of the attractive potentials 0_u^+, 1_u, 0_g^- and 1_g correlated to the $6s + 6p_{3/2}$ limit and of the attractive potentials 0_u^+ and 1_g correlated to the $6s + 6p_{1/2}$ limit. Let us note here that the $0_g^-(6s + 6p_{1/2})$ attractive potential has an asymptotic R^{-6} behavior, which is exceptional for a homonuclear systems.

Two curves correlated to the $6s_{1/2} + 6p_{3/2}$ asymptote, corresponding to 1_u and 0_g^- symmetries, display a double-well structure. The outer well presents a R^{-3} asymptotic behavior and a gentle slope at its inner side. Such double-well structures are due to avoided crossings (due to the large atomic fine structure) between the attractive and repulsive potential curves of given symmetry correlated to the different $6s + 6p_{1/2}$ and $6s + 6p_{3/2}$ limits. They exist for all nuclear dimers, but for the heavier ones (Rb$_2$ and Cs$_2$) the external well is located at an 'intermediate' distance, which, as we shall see, is crucial for the formation of stable ultra-cold molecules.

2. Photoassociation

2.1. Photoassociation rate

The efficiency of the PA process is given by the PA rate for the transition from the molecular ground-state continuum of dissociation up to a ro-vibrational level of an electronically excited potential [2,19,22,23], whose expression is similar to the result of a Fermi golden rule

$$R_{PA} = \frac{N_{at}}{2} \Gamma_{\text{Fermi}} = \frac{N_{at}}{2} \frac{2\pi}{\hbar} |W_{eg}|^2 \rho(E_e - E_g - h\nu_{PA}), \tag{2}$$

where $\rho(\Delta) = (h^3/V)(\beta/(2\pi\mu))^{3/2}\,\mathrm{e}^{-\beta\hbar\Delta}$, with $\Delta = E_e - E_g - h\nu_{PA}$, is the density of states initially populated in the continuum. One has $\beta = 1/k_B T$ and μ is the reduced mass of the molecule. W_{eg} is the matrix element of the Hamiltonian of the electric dipole transition between the initial state and the final state. The PA rate is the number of molecules formed per time unit divided by the number of atoms. It is given by [22]

$$R_{PA} = A(g, e, \vec{\varepsilon}_{PA})\left(\frac{3}{2\pi}\right)^{3/2}\frac{h}{2}n_{at}\lambda_{th}^3\exp(-\Delta/k_B T)K^2|S(\alpha,v)|^2, \tag{3}$$

where $A(g, e, \vec{\varepsilon}_{PA})$ is an angular factor depending on the initial state g, on the final state e, and on the laser polarization $\vec{\varepsilon}_{PA}$: in our experiments it is typically of the order of 10^{-2} [24]. $\lambda_{th} = h\sqrt{\mu k_B T/3}$ is the thermal de Broglie wavelength. The atomic Rabi frequency, $2K$, can be deduced from

$$K^2 = \frac{\Gamma^2}{2}\frac{I}{I_0}. \tag{4}$$

The saturation intensity $I_0 = (\pi h c\Gamma/3\lambda_{PA}^3)$ has a value 1.1 mW/cm^2 in the case of the cesium ($\Gamma/2\pi = 5.22$ MHz is the natural width of the atomic $6p$ level, λ_{PA} is the wavelength of the PA process). The PA rate depends on the overlap integral $S(\alpha, v) = \langle\alpha|v\rangle$ between the (energy-normalized) radial wavefunction of the initial continuum state α, and the bound wavefunction of the final vibrational level v. For long-range excitation (corresponding to large v) the Franck–Condon factor $|S(\alpha, v)|^2$ is, to very good approximation, proportional to $|\psi_\alpha(R_T)|^2$, the square of the modulus of the radial wavefunction ψ_α of the two colliding atoms taken at the classical outer turning point, R_T, of the final ro-vibrational level. We thus expect important variations in the PA rate, with quasi-zero efficiency when the classical outer turning point, R_T, corresponds to a node of the radial wavefunction, ψ_α [25]. Fig. 6 in the reference [24] gives a typical example for calculated PA rates and shows the quantity R_{PA} as a function of the detuning for the attractive molecular potentials correlated to the asymptotic limits $6s_{1/2} + 6p_{1/2 \text{ or } 3/2}$ with the 0_g^- and 0_u^+ symmetries. Within our experimental conditions (more generally with alkali atoms in a vapor-cell magneto-optical trap), one obtains typically a PA rate of one molecule per atom and per second.

The dynamic trap equation expressing the balance between the loading rate L and the various trap loss rates, initially for a total number of trapped atoms N_{at} and a density n_{at} can be written

$$\frac{\mathrm{d}N_{at}}{\mathrm{d}t} = L - \gamma N_{at} - (\beta + \beta_{PA})\int_{\text{vol}} n_{at}^2(r)\,\mathrm{d}^3r, \tag{5}$$

where γ, β and β_{PA} are respectively the loss rates due to background gas collisions, to binary collisions and to PA collisions among the trap atoms. One has the relation $R_{PA} \approx n_{at}\beta_{PA}$. Illumination of the trapped atoms with the PA laser gives rise in the steady regime to a decrease of the number of atoms from N_{at} to N_{PA} with

$$\frac{N_{PA}}{N_{at}} \simeq \frac{\gamma + \beta n_{at}}{\gamma + (\beta + \beta_{PA})n_{at}}. \tag{6}$$

Trap-losses from a few percent up to nearly 100% can be observed and permit a determination of the PA rates. Comparison between experimental and calculated rates are in good agreement [24]. Trap-loss spectroscopy is the detection used in most PA experiments. Fluorescence spectra are recorded by scanning the PA laser frequency. The presence of a dip corresponds generally to a PA reaction followed by a spontaneous photodissociation process where the pair of atoms possesses a relative kinetic energy large enough (typically 1 K) for the two atoms to escape outside of the trap. The formation of cold molecules, through bound–bound transition from the selected PA level towards levels in the ground state, is generally negligible.

2.2. Formation of cold molecules

The possibility to form ultracold molecules in the ground state after spontaneous emission by the excited photoassociated molecules, although it is usually negligible, is quite a fascinating consequence of the PA process. It requires in fact an exceptionally favorable branching ratio between bound-free transitions (leading to dissociation of the molecules) and bound–bound ones (leading to formation of cold molecules) from the excited molecules reached by PA. For long-range molecules corresponding to a single-well molecular potential, this branching ratio is generally very small. During their vibrational motion, the two nuclei of the excited molecule formed by PA are most of the time very far from each other, too far for spontaneous emission to occur at short enough interatomic distance (see arrow (i) of Fig. 1). The situation is totally different when the long-range molecules formed by PA correspond to the outer well of a double-well potential. The vibrational motion corresponds here to an acceleration from the outer classical turning point up to the middle potential bump, at intermediate distance, where the mutual motion of the atoms is slowed down on the gentle inner edge of the outer well. There exists thus in this region a so-called Condon point with a reasonable probability to observe a bound–bound transition in the decay process (see arrows (ii)
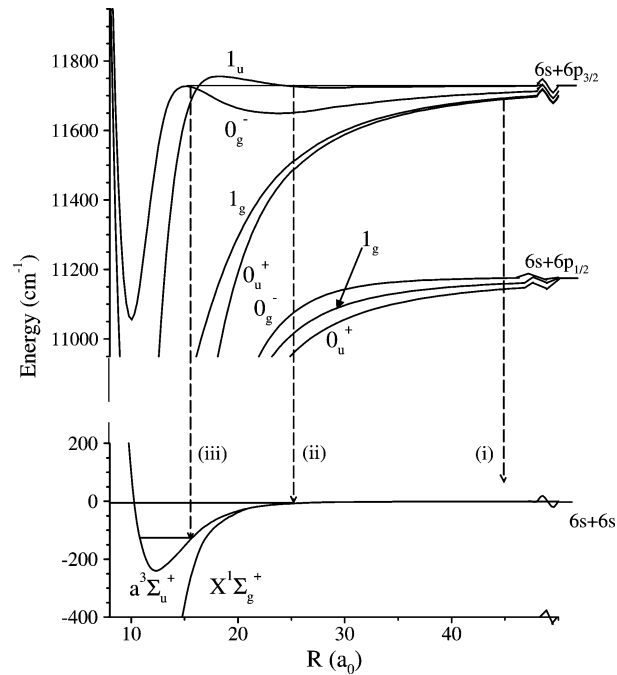
Fig. 1. Potential curves for the $6s + 6s$ and $6s + 6p$ dissociation limits of Cs_2. These curves are obtained by matching short range ab initio calculations [39] with long-range ones.

and (iii) of Fig. 1). The case of the outer wells of 1_u and 0_g^- $(6s + 6p_{3/2})$ for Rb_2 or Cs_2 is therefore ideal for the formation of ultracold molecules in the ground state or in the lowest triplet state. There are other possibilities, but in this paper we will limit ourselves to analyzing the spectroscopic possibilities offered by these two states.

3. Photoassociation spectroscopy

3.1. One-photon spectroscopy

Typical data are shown in Fig. 2 for a range 0–80 cm^{-1} below the $(6s + 6p_{3/2})$ dissociation limit of the PA laser detuning. Two kind of spectra are reported. The upper curve is the fluorescence spectrum, whereas the lower shows the Cs_2^+ ion spectrum, corresponding to laser photoionization of the cold molecules formed either in the ground singlet state or in the lowest triplet state.The fluorescence spectrum shows the ro-vibrational progressions for the attractive potential states 0_u^+, 0_g^- and 1_g. The progression due to the 1_u state is not present in the fluorescence spectrum because of the small depth (< 8 cm^{-1}) of this potential: dissociation of photoassociated molecules leads thus to pairs of atoms with small kinetic energy, which are trapped again by the MOT. Indeed the kinetic energy of a vibrational level v, with energy E_v, of a diatomic molecule is given by [26]

$$E_{\text{kin}} \approx \frac{1}{2}\left(v + \frac{1}{2}\right)(E_{v+1} - E_v). \tag{7}$$

This explains why the 1_u states do not appear in the trap loss signal. Conversely, as the ion signal is due to stable molecule formation, the ion spectrum shows only the vibrational progressions of the 0_g^- and 1_u states.

To identify the vibrational progressions, we used first the calculated width due to the hyperfine structure which allows one to identify each electronic excited state and second the LeRoy–Bernstein approach [26,27] which allowed us to extract the experimental effective C_3^{eff} coefficient. We used in fact an improved [28] LeRoy–Bernstein's formula taking into account the nonasymptotic part of the potential curve and also multipolar terms. One of the simplest formula links the energy E_v of the vibrational quantum number v (with respect to its noninteger value v_D at the dissociation energy)

$$D - E_v \approx \left[\sqrt{\frac{\pi}{2\mu}} \frac{\hbar}{(C_3^{\text{eff}})^{1/3}} \frac{\Gamma(4/3)}{\Gamma(5/6)}(v_D - v)\right]^6 + \tilde{\gamma}(v_D - v)^{11}, \tag{8}$$
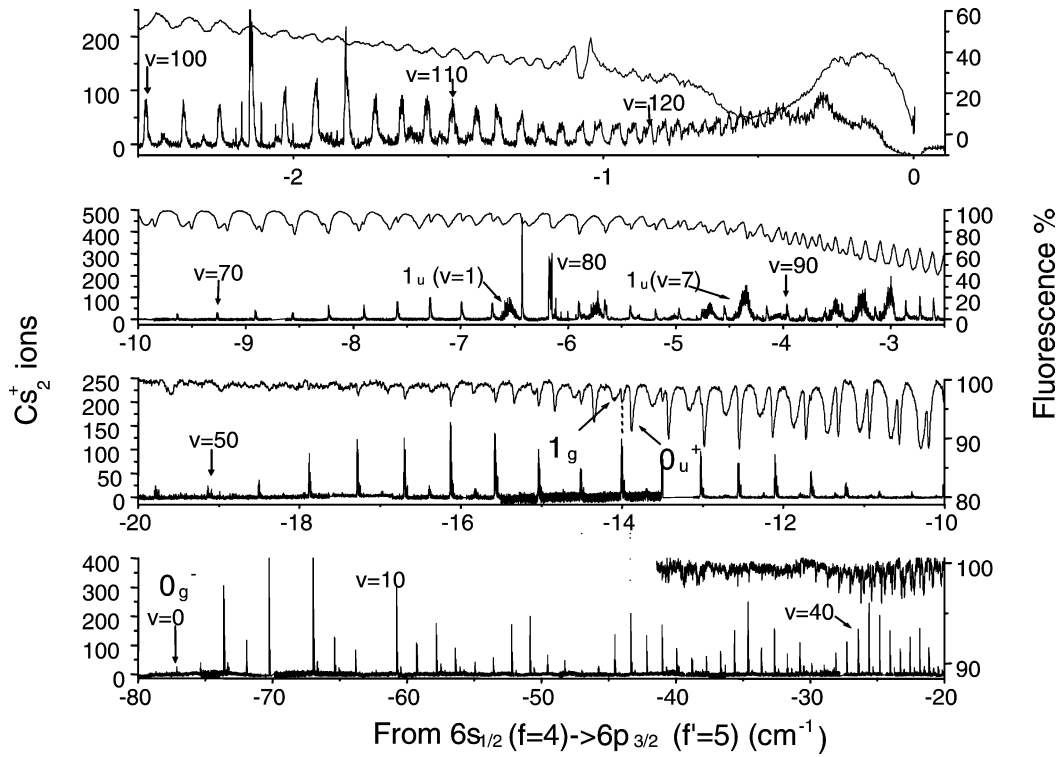
Fig. 2. Cs_2^+ cold molecule ion signal (lower curve) and trap fluorescence yield (upper curve) versus detuning of PA laser below the $6s + 6p_{3/2}$ limit.
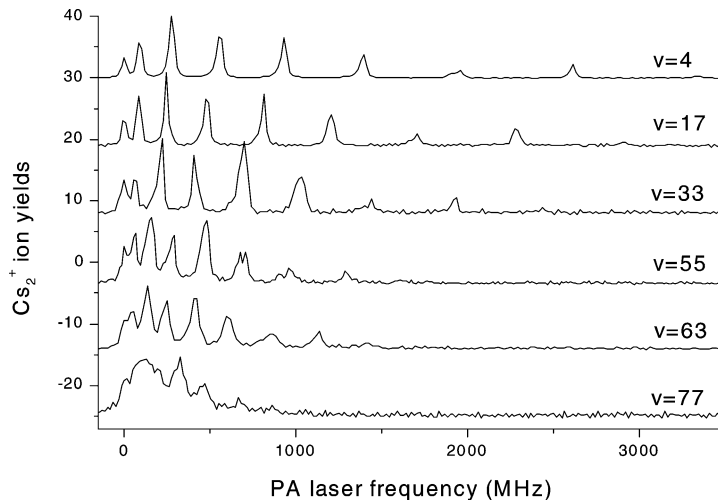

Fig. 3. Rotational structure of different vibrational lines of the 0_g^- potential.

where $\tilde{\gamma}$ takes into account the nonasymptotic part of the potential curve, and where Γ is the gamma function, μ the reduced mass of Cs_2, v_D an effective vibrational noninteger quantum number.

3.1.1. Cs_2 0_g^- pure long-range state

The Cs_2^+ ion spectrum exhibits 133 well resolved structures assigned as the vibrational progression of the 0_g^- state, starting at $v = 0$. Rotational structure, shown for chosen values of v ranging between 4 and 77 in Fig. 3, is resolved up to $J = 8$ for most vibrational levels below $v = 74$. The energies of the spectral lines have been fitted with a Rydberg–Klein–Rees (RKR) and
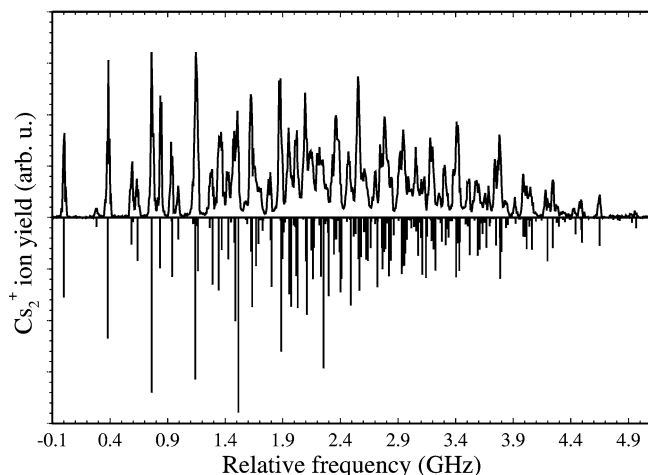
Fig. 4. Mixed rotational and hyperfine structure of the $v = 1$ vibrational level of the 1_u potential. Theoretical results (lower trace) are presented 'in mirror' of the experimental curve (upper trace).

near dissociation expansion (NDE) approach, yielding, for the outer well, an effective potential curve with a 77.94 ± 0.01 cm^{-1} depth and an equilibrium distance $R_e = 23.36 \pm 0.10 a_0$ [29]. This approach provides a good knowledge of the vibrational wavefunctions and of the inner and outer turning points of the classical vibrational motion up to $v = 74$. An approach based on an analytical expression for the external well has also been proposed, yielding values of the atomic radiative lifetimes $\tau_{3/2} = 30.462(3)$ ns and $\tau_{1/2} = 34.88(2)$ ns of the $6p_{3/2}$ and $6p_{1/2}$ atomic levels, with an accuracy better than in previous determinations [30]. We also remark the modulation of the line intensities, which is due to the variations of the Franck–Condon factors of the transitions between the initial state and the final ro-vibrational levels of the 0_g^- state. This modulation can be used for the determination of collisional parameters such as scattering lengths [25,31].

3.1.2. Cs$_2$ 1_u pure long-range state

The large structures in the Cs_2^+ ion spectrum in the range (3–6 cm^{-1}) are assigned to the 1_u state. Fig. 4 shows the well resolved structure of the vibrational level $v = 1$. The spectrum cannot be understood neither as a hyperfine nor as a rotational structure. To interpret these complex structures, we have performed asymptotic calculations including both hyperfine structure and molecular rotation, for all the electronic states involved in 1_u PA [32]. First, a precise calculation of the hyperfine structure of the adiabatic asymptotic potential curves correlated to the excited ($6s + 6p$) asymptotes (without rotation) has been performed, by using the following procedure. We have calculated the matrix elements of the relevant terms of the multipole expansion (R^{-3}, R^{-6}, R^{-8} [33]) and of the fine and hyperfine interactions. We did not introduce exchange energy in the $s + p$ calculations because it is still small at the position of the inner wall of the 1_u potentials (about $25a_0$). As rotation and hyperfine structure are quite entangled (see Fig. 4), we have then made a simultaneous treatment of the two effects. We have diagonalized the sum of the matrix of the asymptotic interaction, taken at a fixed interatomic distance, $R = 32a_0$, i.e., at the bottom of the 1_u potential well, and of the matrix of the operator $B_v \ell^2$, where ℓ is the angular momentum of the relative nuclear motion. B_v is the average value of $1/2\mu R^2$ for the radial wavefunction with vibrational quantum number v, calculated in the 1_u potential previously obtained. A complete calculation of the intensities in which the only adjustable parameters are the initial populations of the different partial waves (from s to g, here), agrees well with experiment (see Fig. 4). Even more than the 0_g^- state, the 1_u state can be said a pure long-range state, consisting of a pair of atoms, the cohesion of which is given by the electrostatic long-range multipole interaction [21].

3.2. Two-photon spectroscopy

The two-color PA process has been described in detail in several articles. Fig. 5 shows the coupling scheme for Λ two-photon PA. The laser L_1 couples a continuum state $|0\rangle$ to a single hyperfine and rotational level labelled $|1\rangle$ of 1_u, $v = 1$ level. The laser L_2 is tuned to probe resonances between $|1\rangle$ and some ro-vibrational Cs$_2$ levels $|2\rangle$ at the ($6s + 6s$) asymptotes. In the absence of any resonant coupling due to L_2, the intermediate level $|1\rangle$ is populated and Cs$_2$ ultracold molecules are formed by PA followed by spontaneous emission. These molecules are detected by photoionization. If a resonance $|1\rangle \rightarrow |2\rangle$ is reached, a dark resonance is formed between $|0\rangle$, $|1\rangle$ and $|2\rangle$, which prevents $|1\rangle$ to be populated and consequently any Cs$_2$ molecule to
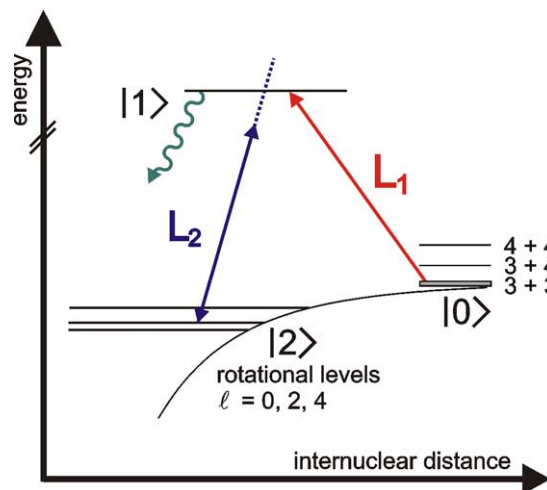
Fig. 5. Coupling scheme for two-photon PA. The two laser fields are noted L_1 and L_2. The excited molecular state is $|1\rangle$ and the one at the ground state asymptote is called $|2\rangle$. The grey shaded area above the lowest hyperfine asymptote represents the thermal distribution of the atoms of the MOT in the continuum states $|0\rangle$.
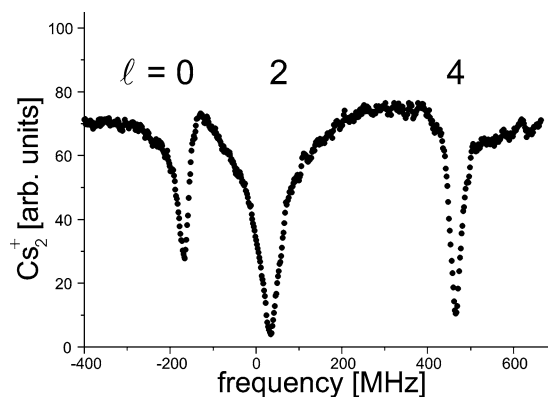
Fig. 6. Example of a rotational series of a vibrational level located about 0.6 cm^{-1} below the lowest hyperfine asymptote. The quantum number ℓ characterizes the rotation of the nuclei.
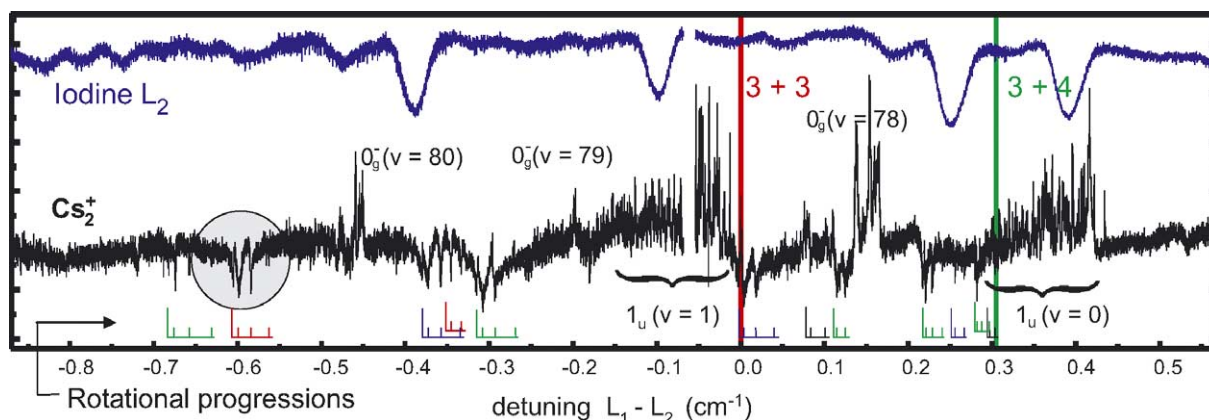

Fig. 7. Overview of a two-photon PA spectrum. The upper trace shows the absorption of the laser L_2 through an iodine cell and is used to roughly calibrate the spectrum. The position of the three hyperfine asymptotes are indicated as vertical lines. Assigned rotational progressions are reported below the spectrum. The shaded area is zoomed in Fig. 6.

be formed. The resonance is therefore observed as a dip in the Cs_2^+ signal as shown in Fig. 6. An overview of the two-color PA spectrum is shown in Fig. 7.

By measuring the positions of levels close to the dissociation thresholds, for which in a classical picture the internuclear distance remains most of the time very large, we investigate in fact the asymptotic region of the lowest electronic states $X^1\Sigma_g^+$ and $a^3\Sigma_u^+$ states of Cs_2. In this region, both states are strongly coupled by the atomic hyperfine interaction, which is very strong in Cs_2 (see, for instance, [34]). For this reason and because of the small vibrational spacing induced by the high mass of Cs, the spectra in the asymptotic region are expected to be dense and difficult to interpret. Details of the interpretation are given in reference [35] and are not reported here. More than 100 asymptotic levels of the coupled electronic states $X^1\Sigma_g^+$ and $a^3\Sigma_u^+$ were identified and measured in a 3.5 cm^{-1} energy interval below the highest hyperfine asymptote. Rotational angular momenta ℓ up to 6 were observed. We have also measured a few levels with energies higher than the lowest hyperfine asymptote, which are subject to predissociation, due to mixing with energetically lower hyperfine channels. The uncertainty of the level energy is of the order of 10 MHz. It includes the uncertainty due to the frequency measurement, the uncertainty of the estimation of the line shift due to thermal distribution of atoms in the MOT and the uncertainty of the determination of the line position, which is limited by the noise of the Cs_2^+ signal [20].

To account for experimental data, it is in general necessary to modify the inner part of the potential, to fit the chosen parameters, and to control the way in which this potential is linked to the asymptotic part of the potential. To avoid these delicate tasks, we have chosen an asymptotic method. By this we mean that the Schrödinger equation is solved in the asymptotic region only, as it was done for instance in [36]. The effect of the inner potential is expressed as boundary conditions on the wavefunctions. More precisely we impose to the wavefunctions to vanish at some nodal lines located near the frontier of the asymptotic region [37]. These nodal lines are used as adjustable parameters which are fitted to the experimental results. In the present case, the data are precise and numerous enough to determine also the main parameters of the asymptotic potential. From this analysis we determined the presently most precise value of the long range dispersion coefficient C_6 of the ground state, which is 6846.2 ± 15.6 atomic units. We also obtained the first experimental determination of the amplitude of the asymptotic exchange term.

4. Conclusion

Photoassociation of ultracold atoms provides a new efficient spectroscopic tool, the precision of which is ultimately given by the width of the thermal distribution of atom velocities. We have shown here, on the example of cesium, how the specific features of this spectroscopy allow us to study long-range molecular states and therefore to study the asymptotic interactions between the atom pairs, at the frontier of atomic and molecular physics. Many new and accurate informations are obtained in this way. PA spectroscopy using atomic BEC reaches ultrahigh resolution [38]. The atomic pairs will then provide a very sensisitive probe for any kind of effects affecting either their internal or their external degree of freedom. This might open to PA spectroscopy some new, still unknown, applications.

References

[1] H.R. Thorsheim, J. Weiner, P.S. Julienne, Laser-induced photoassociation of ultracold sodium atoms, Phys. Rev. Lett. 58 (1987) 2420.
[2] J. Weiner, V.S. Bagnato, S. Zilio, P.S. Julienne, Experiments and theory in cold and ultracold collisions, Rev. Mod. Phys. 71 (1999) 1.
[3] W.C. Stwalley, H. Wang, Photoassociation of ultracold atoms: a new spectroscopic technique, J. Mol. Spectrosc. 195 (1999) 194.
[4] P.D. Lett, K. Helmerson, W.D. Philips, L.P. Ratliff, S.L. Rolston, M.E. Wagshul, Spectroscopy of Na_2 by photoassociation of laser-cooled Na, Phys. Rev. Lett. 71 (1993) 2200.
[5] J.D. Miller, R.A. Cline, D.J. Heinzen, Photoassociation spectrum of ultracold Rb atoms, Phys. Rev. Lett. 71 (1993) 2204.
[6] E.R.I. Abraham, W.I. McAlexander, C.A. Sackett, R.G. Hulet, Spectroscopic determination of the s-wave scattering length of lithium, Phys. Rev. Lett. 74 (1995) 1315.
[7] H. Wang, P.L. Gould, W.C. Stwalley, Photoassociative spectroscopy of ultracold ^{39}K atoms in a high density vapor-cell magneto-optical trap, Phys. Rev. A 53 (1996) R1216.
[8] A. Fioretti, D. Comparat, A. Crubellier, O. Dulieu, F. Masnou-Seeuws, P. Pillet, Formation of Cs_2 cold molecules through photo-association, Phys. Rev. Lett. 80 (1998) 4402.
[9] A.P. Mosk, M.W. Reynolds, T.W. Hijmans, J.T.M. Walraven, Photoassociation of spin-polarized hydrogen, Phys. Rev. Lett. 82 (1999) 307.
[10] N. Herschbach, P.J.J. Tol, W. Wassen, W. Hogervorst, G. Woestenenk, J.W. Thomsen, P. Van der Straten, A. Niehaus, Photoassociation spectroscopy of cold $He(2^3s)$ atoms, Phys. Rev. Lett. 84 (2000) 1874.
[11] J. Léonard, M. Walhout, A.P. Mosk, T. Müller, C. Cohen-Tannoudji, M. Leduc, Giant helium dimers produced by photoassociation of ultracold metastable atoms, Phys. Rev. Lett. 91 (2003) 073203.
[12] G. Zinner, T. Binnewies, F. Riehle, E. Tiemann, Photoassociation of cold Ca atoms, Phys. Rev. Lett. 85 (11) (2000) 2292.
[13] J.P. Shaffer, W. Chalupczak, N.P. Bigelow, Photoassociative ionization of heteronuclear molecules in a novel two-species magneto-optical trap, Phys. Rev. Lett. 82 (6) (1999) 1124.
[14] U. Schlöder, C. Silber, C. Zimmermann, Photoassociation of heteronuclear lithium, Appl. Phys. B 73 (2001) 801.
[15] A.J. Kerman, J.M. Sage, S. Sainis, D. DeMille, T. Bergeman, Production of ultracold polar RbCs* molecules via photoassociation, Phys. Rev. Lett. 92 (2004) 033004.
[16] A.N. Nikolov, J.R. Enscher, E.E. Eyler, H. Wang, W.C. Stwalley, P.L. Gould, Efficient production of ground state potassium molecules at sub-mK temperatures by two-step photoassociation, Phys. Rev. Lett. 84 (2000) 246.
[17] C.C. Tsai, R.S. Freeland, J.M. Vogels, H.M.J.M. Boesten, J.R. Gardner, D.J. Heinzen, B.J. Verhaar, Two-color photoassociation spectroscopy of ground state Rb_2, Phys. Rev. Lett. 79 (1997) 1245.
[18] B. Laburthe Tolra, C. Drag, P. Pillet, Observation of cold state-selected cesium molecules formed by stimulated Raman photoassociation, Phys. Rev. A 64 (2001) 61401(R).
[19] J.L. Bohn, P.S. Julienne, Semianalytic theory of laser-assisted cold collisions, Phys. Rev. A 60 (1) (1999) 414.
[20] Ch. Lisdat, N. Vanhaecke, D. Comparat, P. Pillet, Line shape analysis of two-colour photoassociation spectra on the example of the Cs_2 ground state, Eur. Phys. J. D 21 (2002) 299–309.
[21] W.C. Stwalley, Y. Uang, G. Pichler, Pure long-range molecules, Phys. Rev. Lett. 195 (1978) 194–228.
[22] P. Pillet, A. Crubellier, A. Bleton, O. Dulieu, P. Nosbaum, I. Mourachko, F. Masnou-Seeuws, Photoassociation in a gas of cold alkali atoms. I: Perturbative quantum approach, J. Phys. B 30 (1997) 2801.

[23] R. Côté, A. Dalgarno, Mechanism for the production of vibrationally excited ultracold molecules of $^7Li_2$, Chem. Phys. Lett. 279 (1997) 50.

[24] C. Drag, B. Laburthe Tolra, O. Dulieu, D. Comparat, M. Vatasescu, S. Boussen, S. Guibal, A. Crubellier, P. Pillet, Experimental versus theoretical rates for photoassociation and for formation of ultracold molecules, IEEE J. Quant. Electron. 36 (2000) 1378.

[25] C. Drag, B. Laburthe Tolra, B. T'Jampens, D. Comparat, M. Allegrini, A. Crubellier, P. Pillet, Photoassociative spectroscopy as a self-sufficient tool for the determination of the cs triplet scattering length, Phys. Rev. Lett. 85 (2000) 1408.

[26] W.C. Stwalley, Expectation values of the kinetic and potential energy of a diatomic molecule, J. Chem. Phys. 58 (1973) 3867.

[27] R.J. LeRoy, R.B. Bernstein, Dissociation energy and long-range potential of diatomic molecules from vibrational spacings of higher levels, J. Chem. Phys. 52 (1970) 3869.

[28] D. Comparat, Improved LeRoy–Bernstein near-dissociation expansion formula, and prospect for photoassociation spectroscopy, J. Chem. Phys. 120 (2004) 1318.

[29] A. Fioretti, D. Comparat, C. Drag, C. Amiot, O. Dulieu, F. Masnou-Seeuws, P. Pillet, Photoassociative spectroscopy of the $Cs_2 \, 0_g^-$ long-range state, Eur. Phys. J. D 5 (1999) 389.

[30] C. Amiot, O. Dulieu, R.F. Gutteres, F. Masnou-Seeuws, Determination of the $Cs_2 \, 0_g^- \, (p_{3/2})$ potential curve and the Cs $6p_{1/2,3/2}$ atomic radiative lifetimes grom photoassociation spectroscopy, Phys. Rev. A 66 (2002) 052506.

[31] E. Tiesinga, C.J. Williams, P.S. Julienne, K.M. Jones, P.D. Lett, W.D. Phillips, A spectroscopic determination of scattering lengths for sodium atom collisions, J. Res. Inst. Stand. Technol. 101 (1996) 505.

[32] D. Comparat, C. Drag, B. Laburthe Tolra, A. Fioretti, P. Pillet, A. Crubellier, O. Dulieu, F. Masnou-Seeuws, Formation of cold Cs_2 ground state molecules through photoassociation of the 1_u long-range state, Eur. Phys. J. D 11 (2000) 59.

[33] M. Marinescu, A. Dalgarno, Analytical interaction potentials of the long range alkali-metal dimers, Z. Phys. D 36 (1996) 239–248.

[34] H. Weckenmeier, U. Diemer, W. Demtröder, M. Broyer, Hyperfine interaction between the singlet and triplet ground states of Cs_2: a textbook example of gerade-ungerade symmetry breaking, Chem. Phys. Lett. 124 (4) (1986) 470.

[35] N. Vanhaecke, Ch. Lisdat, B.T'Jampens, D. Comparat, A. Crubelleier, P. Pillet, Accurate asymptotic ground state potential curves of Cs_2 from two-colour photoassociation, Eur. Phys. J. D (2004), in press.

[36] J.M. Vogels, R.S. Freeland, C.C. Tsai, B.J. Verhaar, D.J. Heinzen, Coupled singlet-triplet analysis of two-color cold-atom photoassociation spectra, Phys. Rev. A 61 (2000) 043407.

[37] A. Crubellier, O. Dulieu, F. Masnou-Seeuws, M. Elbs, H. Knöckel, E. Tiemann, Simple determination of Na_2 scattering lengths using observed bound levels at the ground state asymptote, Eur. Phys. J. D 6 (1999) 211–220.

[38] R. Wynar, R.S. Freeland, D.J. Han, C. Ryu, D.J. Heinzen, Molecules in a Bose–Einstein condensate, Science 287 (2000) 1016.

[39] N. Spiess, Ph.D. thesis, Fachbereich Chemie, Universität Kaiserslautern, 1989.